Geomechanics and Engineering, *Vol. 34, No. 1 (2023) 51-67*
https://doi.org/10.12989/gae.2023.34.1.051

Assessing the long-term durability and degradation of rocks under freezing-thawing cycles

Seyed Zanyar Seyed Mousavi[a] and Mohammad Rezaei*

Department of Mining Engineering, Faculty of Engineering, University of Kurdistan, Sanandaj, Iran

(*Received May 23, 2022, Revised May 2, 2023, Accepted May 11, 2023*)

Abstract. In this research, the degradation rate of physical properties of the Angouran pit bedrock (calc-schist) is first investigated under the specific numbers of freeze-thaw (F-T) cycles. Then, the durability of calc-schist specimens against the F-T cycle number (N) is examined considering the mechanical parameters, and using the decay function and half-time techniques. For this purpose, point load strength ($I_{S(50)}$), second durability index (I_{d2}), Brazilian tensile strength (BTS), and compressive (V_P) and shear (V_S) wave velocities of calc-schist specimens are measured after 0, 7, 15, 40, and 75 N. For comparing the degradation rate of mechanical properties of available rock types on the Angouran mine walls, these tests are also carried out on the limestone and amphibolite schist specimens beside the calc-schist. According to test results, the exponential regression models are developed between the mechanical parameters of rock specimen's and N variable. Also, the long-term durability of each rock type versus N is studied using the decay function and half-time techniques. Results indicated that the degradation rate differs for the above rock types in which amphibolite schist and calc-schist specimens have the highest and least resistance against the N, respectively. The obtained results from this study can play a key role in the optimal design of the mine's final walls.

Keywords: angouran mine; bedrock properties; decay function; freeze-thaw cycle; half-time; laboratory test

1. Introduction

The freeze-thaw (F-T) process is an important phenomenon that can deteriorate the physical and mechanical characteristics of soils, rocks, and concretes. In the last decade, the construction of engineering projects such as dams, tunnels, and mines have been widely developed in cold regions. Due to the repetition of F-T cycles in these regions, degradation process causes soil/rock/concrete failure and bedrock landslide. Consequently, the bedrock durability of these projects decreases due to the degradation of rock mass characteristics and affects the stability and safety of the engineering construction (Ruedrich *et al.* 2011, Yilmaz and Fidan 2018, Moon *et al.* 2022). By decreasing the temperature, existing water inside the available pores and discontinuities in the rock body was frozen, and its volume expanded and lead to the further pressure on the walls of discontinuities. When this pressure exceeds the rock tensile strength, new micro-cracks are created, and existing cracks and pores are expanded gradually (Takarli *et al.* 2008, Wang *et al.* 2016, Huang *et al.* 2018, Zhang *et al.* 2020, Tang *et al.* 2021, Cheng *et al.* 2021).

In the recent years, few studies have been conducted on the reduction of physical and mechanical characteristics of rocks due to weathering agents (Karaca *et al.* 2010, Uğur and Toklu 2020). Binal *et al.* (1998) studied the impact of N on the physical and mechanical properties of ignimbrite. Altindag *et al.* (2004) examined the reduction rate of the ignimbrite mechanical characteristics using the suggested decay function technique by Mutlutürk *et al.* (2004). Yavuz *et al.* (2005) presented a new equation to estimate the changes in key characteristics of carbonate samples due to the F-T process. Tan *et al.* (2011) examined the variations of unconfined compressive strength (UCS) of granite due to the F-T process and showed that UCS is reduced exponential with N increasing. Khanlari and Abdilor (2015) evaluated the F-T process effect on porosity, compressional wave velocity (V_p), and UCS of sandstone. Results indicated that porosity was increased after F-T process cycles, whereas V_p and UCS were reduced. The degradation of sandstone under the effect of N and chemical devolution was evaluated by Han *et al.* (2016). Jamshidi *et al.* (2016) studied the durability of Gerdoee travertine against the F-T processes in freshwater and sodium sulfate liquid using the decay function model. Ke *et al.* (2018) proposed a practical model to evaluate the degradation of sandstone mechanical characteristics due to the F-T process. Seyed Mousavi *et al.* (2019) estimated the influence of the F-T process on the outputs of the triaxial compressive test (TCS) test of calc-schist rock samples. Seyed Mousavi *et al.* (2020) investigate the changes in structural, petrological, and mechanical characteristics of schist samples under the influence of the F-T process. They concluded that the mechanical characteristics of considered rock samples are exponentially reduced with increasing the N. Liu *et al.* (2020) studied the changes in granite rock structure due to the F-T process under the size influence. They found that the macro-pores and porosity are increased with increasing

*Corresponding author, Associate Professor
E-mail: m.rezaei@uok.ac.ir
[a]Ph.D.
E-mail: z.mousavi@uok.ac.ir

ISSN: 2005-307X (Print), 2092-6219 (Online)

the N and sample size. The shear resistance of the sandstone-cement interface under the N effect was investigated by Wang *et al.* (2020) and they concluded that increasing the N causes the increasing of specimens' shear resistance degradation. Seyed Mousavi and Rezaei (2022) evaluated the correlation of the UCS degradation ratio with non-destructive properties of rock under F-T cycles. Finally, Sardana *et al*. (2022) were done an extensive work on the degradation of the physical and mechanical properties of Himalayan rocks due to the freezing and thawing process.

Taking into account the results of the above reviewing references, it can be concluded that a deep understanding of changes in geo-mechanical characteristics of rocks due to F-T cycles is a valuable task in designing engineering projects constructed in mountainous and cold regions**.** Indeed, the F-T process affected the durability of rock mass and causes instability of bedrock construction. In the last decade, metamorphic rocks (especially schist rocks) have received less attention by researchers, and thus; there is very limited information in the reviewed literature in this regard. On the other hand, precise determination of the geomechanical properties of existing rock masses is essential to design a stable slope in open pit mines. However, weathering agent reduces the physical and mechanical parameters of rock units. Therefore, estimating the degradation rate of these characteristics of rock mass is a crucial factor in accurately designing the overall slope angle in an open pit mine. The main reason for limited studies in the field of metamorphic rocks may be due to the core crushing because of schistosity and discontinuity planes during the drilling operation. Meanwhile, the bedrock of a significant number of engineering projects consists of metamorphic rocks**.** One of the main factors for the landslide and slope instability in these bedrocks type is the presence of schistosity in their bodies. As weathering process affects the strength properties of schistosity and other physico-mechanical characteristics of metamorphic rocks, so impacts of N on the physical characteristics of calc-schist have been first evaluated in this research. Next, the long-term durability of calc-schist, limestone, and amphibolite schist under different F-T cycles is investigated using the decay function technique suggested by Mutlutürk *et al.* (2004) considering the Brazilian tensile strength, second slake durability index, point load strength, compressive strength, P-wave velocity, and S-wave velocity parameters.

2. Case study

In this study, the three rock samples required for conducting the considered experimental tests were prepared from the Angouran open-pit mine area. This case study is situated in the northwest part of Iran (Fig. 1). The mine is 2900 m above the sea in its highest part. The ore body is located between the calc-schist and amphibolite schist rocks as the footwall and limestone formation as the hanging wall side (Fig. 2). Continuous extraction of the Angouran mine is critical for Iran as it supplies the feeds of many factories (Rezaei and Ghasemi 2023). Therefore, taking into consideration the region's climate, investigations into the effect of atmospheric factors in the stability analysis of mine rock walls are essential. For this purpose, 13 boreholes were identified and drilled in the mine area (Fig. 3). To reduce the individual differences of samples (due to the existence of anisotropy) and to achieve high-accuracy laboratory results, drilling operations are performed vertically and additional core specimens were retrieved.

2.1 Weathering process

Schist weathering is the major weathering process in the Angouran mine. In this mine, the F-T process and the chemical weathering have affected the intersection of bedrock and limestone and inside the faults (effect of alteration in the intersection of calc-schist and limestone). As a result, it leads to the degradation of the physico-mechanical properties of calc-schist rock which encompasses the main final wall of the mine. The annual movement of wall schist rock to the mine floor imposed high costs on the mining operations. This degradation commonly occurs due to the weathering process that affects the properties of existing structures (including foliation, schistosity, and discontinuity) and the mineralogical composition of the calc-schist rock. Intact, water freezing induces tensile forces in the discontinuity walls and causes the creation of new micro-cracks and expanding the existing cracks. Moreover, the repetition of this process increases the density of discontinuities. Besides, in terms of mineralogy, calcite is one of the main constitutive minerals of calc-schist that has highly expandable properties. Due to the existing of high amounts of calcite in the calc-schist context, it may be degraded because of the calcite expansion. According to the comprehensive field and laboratory inspections, it was observed that both the mineralogical composition and structural properties of calc-schist samples together affect the strength and durability of this rock. Due to this fact, weathering agents and degradation rate are very high in calc-schist rock. In practice, the mentioned factors affect the durability of calc-schist and increase the displacement of this rock in the western wall of the Angouran mine, which imposes a high cost on the mining operation because of the additional stripping. Changes in temperature during different seasons and day-night cycles in the Angouran mine are shown in Table 1 which demonstrated the significance of weathering process in the mine area.

According to drilled boreholes in the western wall of mine and its benches face, its lithology consists of 10-15 m of highly weathered calc-schist, as well as 40-60 m of moderately weathered and intact calc-schist from the end of the second layer to depth, respectively (Figs. 4 and 5). In highly weathered materials, quartz grains are fractured while biotite and chlorite are exfoliated and mainly oxidized on the surface of cleavage planes. In moderately weathered material, biotites and chlorites are exfoliated and mainly oxidized on the surface of cleavage planes. Generally, the effect of weathering agent on the rock mass in this study area is superficial. Indeed, the weathered zone has about an average thickness of 2 m.

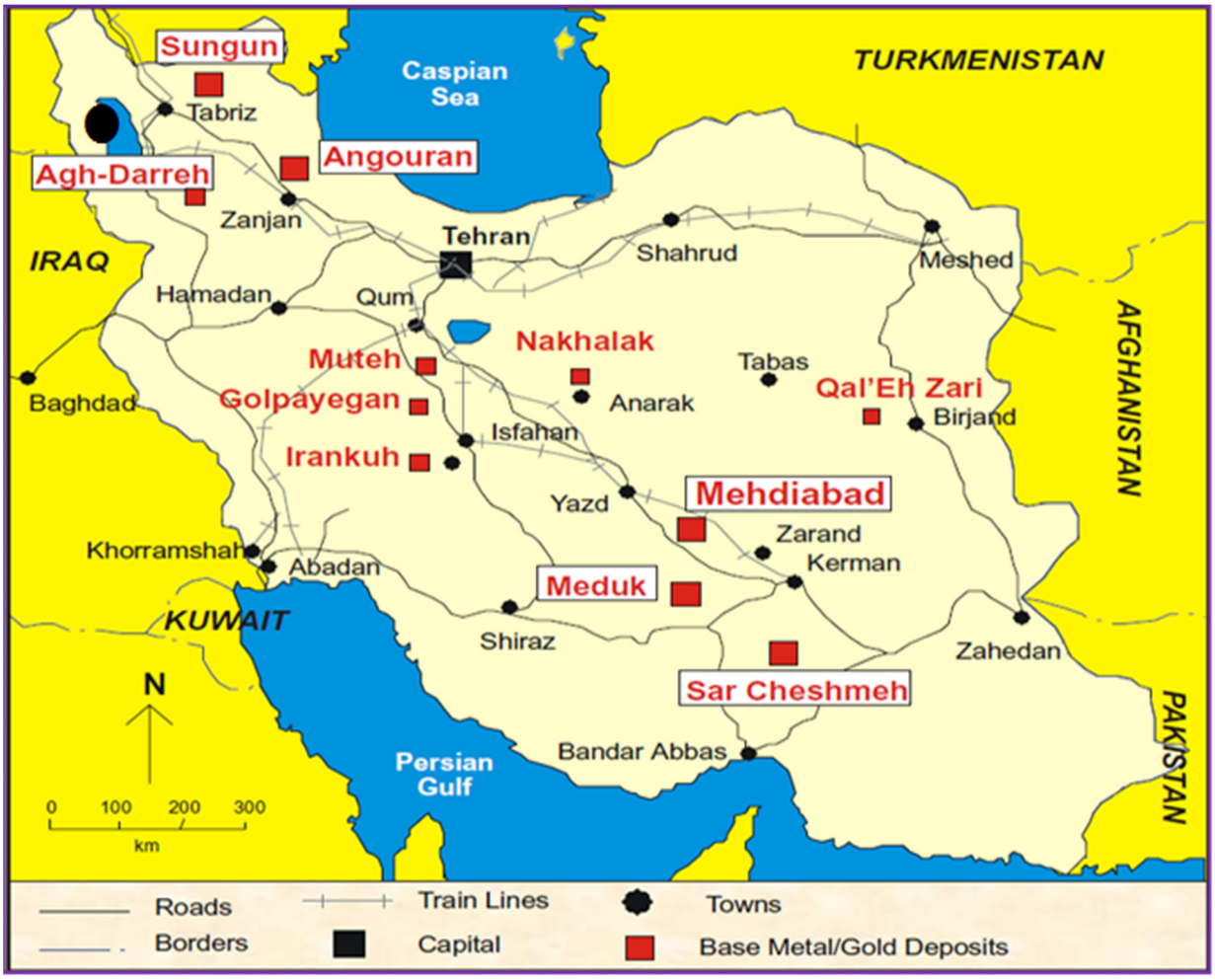

(a)

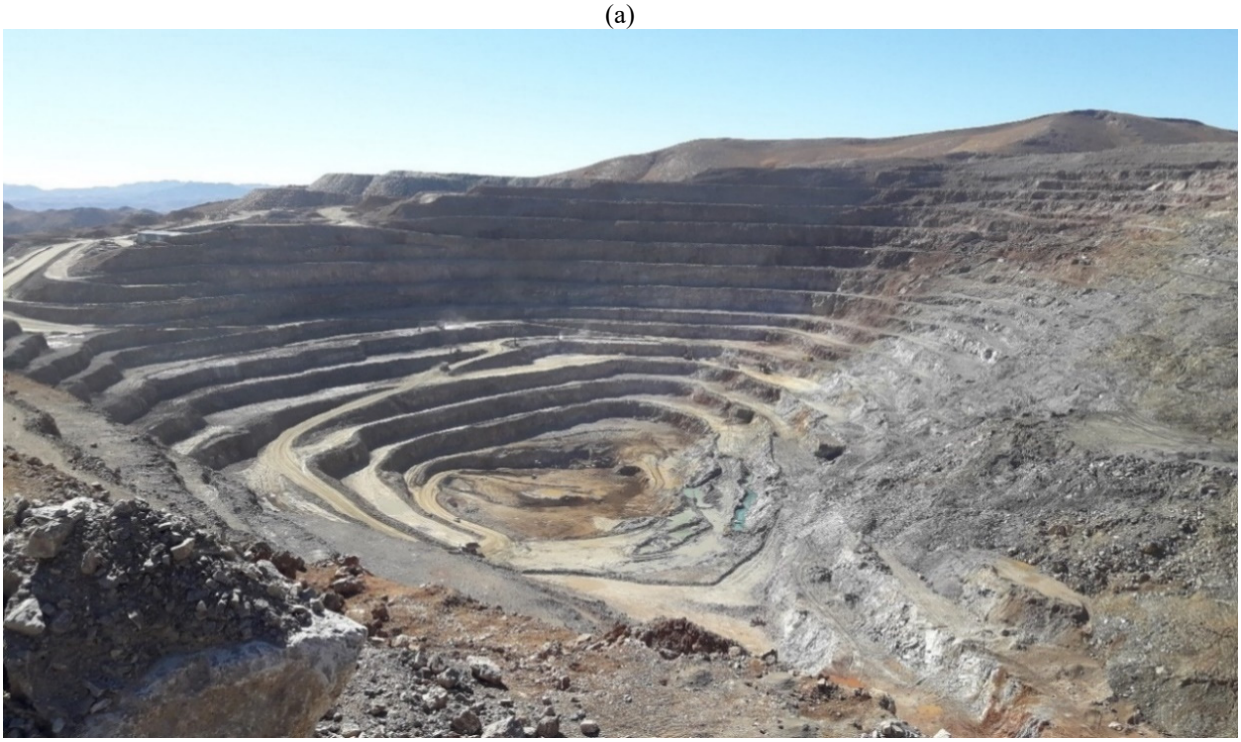

(b)

Fig. 1 (a) Location of the Angouran open-pit mine and (b) Situation of mine benches

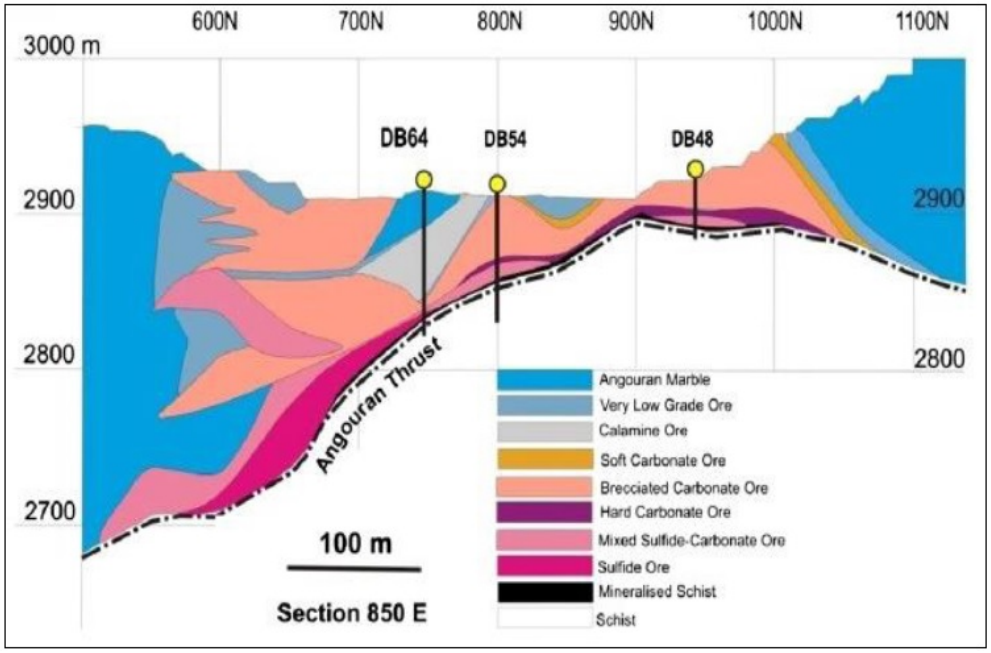

Fig. 2 The geological cross-section (north-south) of the Angouran mine

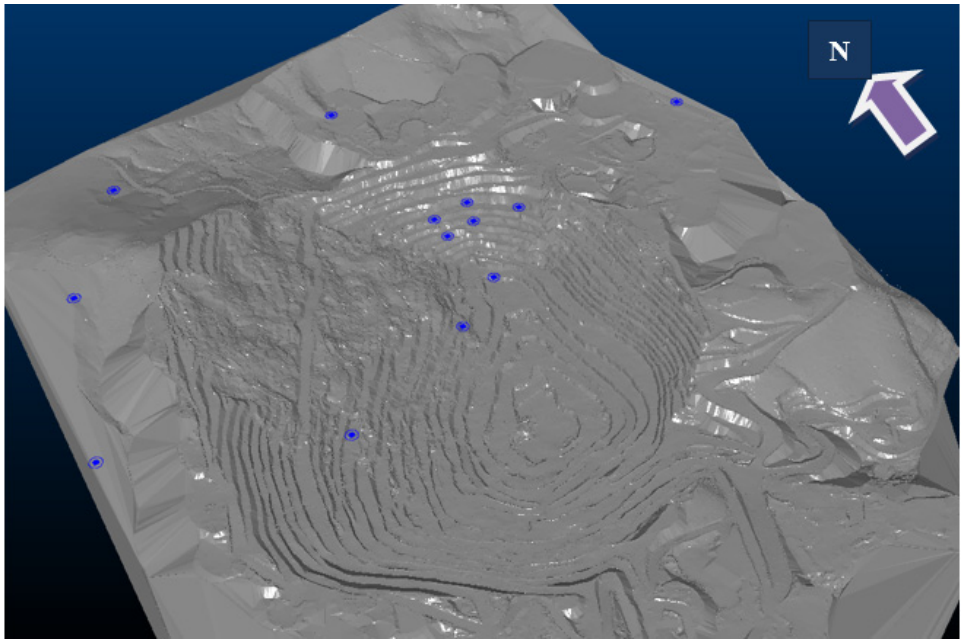

Fig. 3 Position of excavated boreholes at the mine area

Table 1 Changes of the temperature for different seasons and day/night period

Spring	Day	12°C
	Night	-2°C
Summer	Day	20°C
	Night	4°C
Autumn	Day	14°C
	Night	-8°C
Winter	Day	10°C
	Night	-20°C

3. Materials and methods

In this section, experimental measurements of the physical and mechanical characteristics of rock samples are outlined. The experiments were conducted based on the related techniques recommended by ISRM (1981), ASTM (2001), and ISRM (2007). Detailed descriptions of these experiments are found in the kinds of literature (Rezaei 2018, 2020, Rezaei *et al.* 2019, Rezaei and Asadizadeh 2020, Asadizadeh and Rezaei 2021, Rezaei and Nyazyan 2023) and thus, they will be described here briefly.

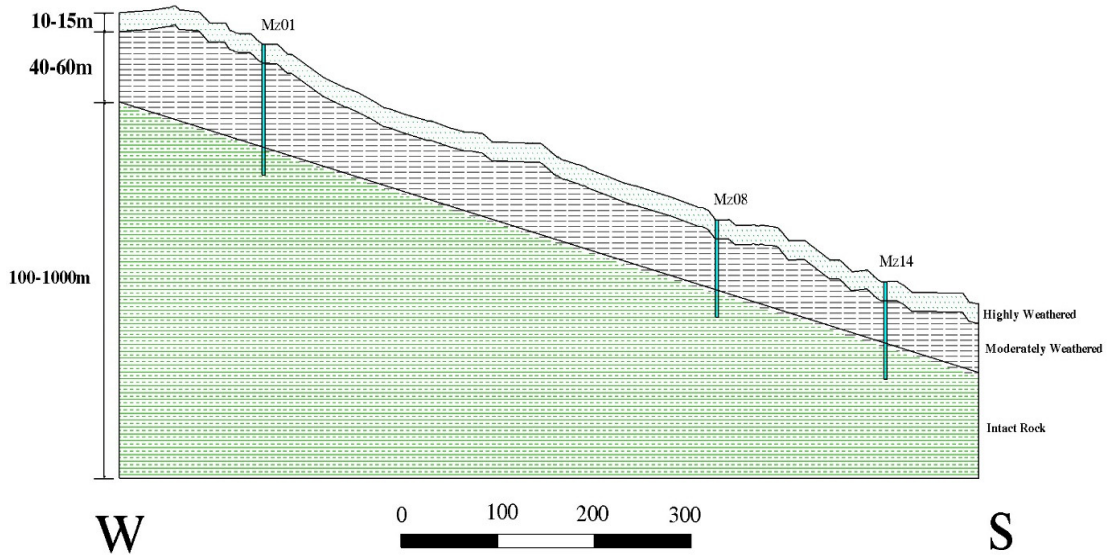

Fig. 4 Position of excavated boreholes at the mine area

3.1 Dry density

In this study, the dry density of cylindrical rock samples was measured based on the proposed approach by ISRM (1981). The dry density (γ_{dry}) of five samples were measured after 0, 7, 15, 40, and 75 cycles of F-T, according to Eq. (1).

$$\rho_{dry} = \frac{M_{dry}}{V_{dry}} \tag{1}$$

where M_{dry} and $V_{dry}$are the mass and volume of dried samples, respectively.

3.2 Slake durability index

According to Gamble (1971), the second cycle of slake durability index (I_{d2}) is the best durability indicator of rocks and thus it was measured in the current study. To carry out the durability test, 10 pieces of 50±5 grams of rock samples with a total mass of 500 grams are prepared based on the procedure proposed by the ISRM (1981). Here, the I_{d2} was determined according to the suggested approach by Franklin and Chandra (1972).

3.3 Water absorption

Water absorption tests were performed on the rock pieces ranging from 20 mm to 63 mm in size amounts. The water absorption test can be used as a basic tool for evaluating the durability of rock. In this study, water absorption of calc-schist rock is determined for 5 cylindrical core specimens after 0, 7, 15, 40, and 75 cycles according to the ASTM (2001) and using Eq. (2).

$$A_w = \frac{M_s - M_d}{M_d} \times 100\% \tag{2}$$

where M_s and M_d are the mass of saturated/soaked and dried specimens, respectively.

3.4 Brazilian tensile strength

This test is commonly carried out on rock cylindrical specimens according to the ISRM (1981). Samples are prepared with 63 mm diameter (D) and a ratio of length to diameter (L/D) of 0.5. The test was carried out using the Instron 8502 servo-hydraulic substances experiment device. In this system, the tensile force is employed continuously to the studied sample by applying a constant force such that the sample failure occurs during 5 min of loading. After the corresponding cycle of F-T, the tensile strength (σ_t) of 5 samples was measured using Eq. (3).

$$BTS = \frac{2L}{\pi Dt} \tag{3}$$

where L, D, and t are the length, diameter, and thickness of samples.

3.5 Ultrasonic wave velocity

The ultrasonic wave velocities (P and S types) of cylindrical rock samples were measured in this research. Rock specimens were prepared in 63 mm diameter and 150 mm length. Also, the end of the sample was polished and made perpendicular to the axis. In this work, two transducers with a frequency of 54 kHz were used as a receiver and PUNDIT instrument was applied as a transmitter. Wave velocities were calculated based on travel time through the samples. It should be noticed that the test was performed after applying the previously defined F-T cycles on the mentioned five specimens.

3.6 Porosity

The rock porosity was commonly classified into total porosity, effective porosity, and open porosity. In this research, the total porosity (ϕ) of samples was determined according to the ISRM (2007) using Eq. (4).

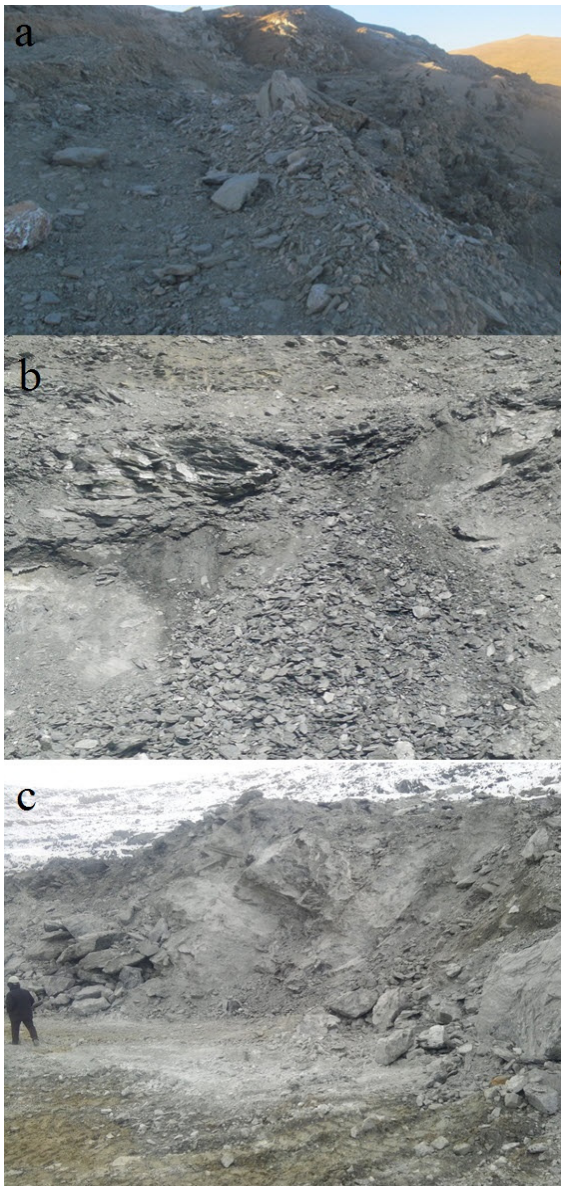

Fig. 5 Calc-schist weathering grade in the western wall of Angouran mine (a): highly weathered, (b) moderately weathered, and (c) intact)

$$\phi = \frac{M_s - M_d}{M_s - M_w} \times 100\% \quad (4)$$

where M_s is the saturated/soaked specimen mass, M_w is the water mass, and M_d is the dried sample mass.

3.7 Point load strength

In this study, the point load experiment was utilized to evaluate other strength parameters that can be correlated with the σ_t and UCS. This test is routinely performed in different shapes of specimens and directions i.e., irregular specimens, axial tests, and diametrical tests. In this research, the diametric point load experiment was conducted to specify the point load strength of core samples with 63 mm diameter and 55 mm length. The measured outputs were modified to calculate the point load strength of a sample with a 50 mm diameter ($I_{S(50)}$). The point load strength experiment was carried out on 5 samples after

(a)

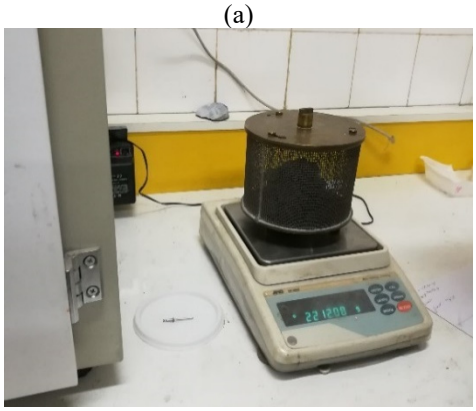

(b)

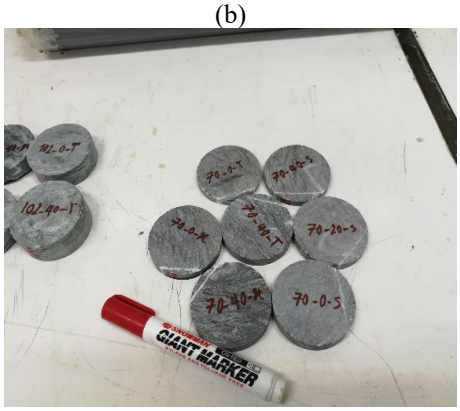

(c)

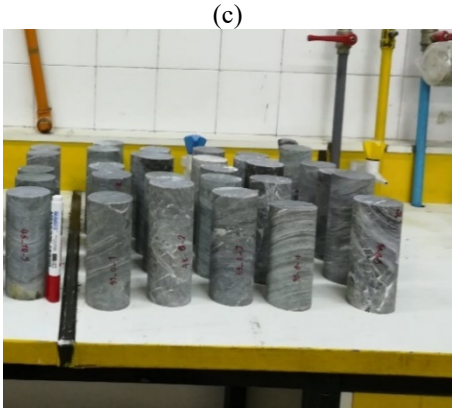

(d)

Fig. 6 Prepared samples to carry out the experimental tests: (a) & (b) Slake durability samples, (c) Thin section samples and (d) Ultrasonic wave velocity samples

Fig. 7 Condition of the Angouran mine in a cold season

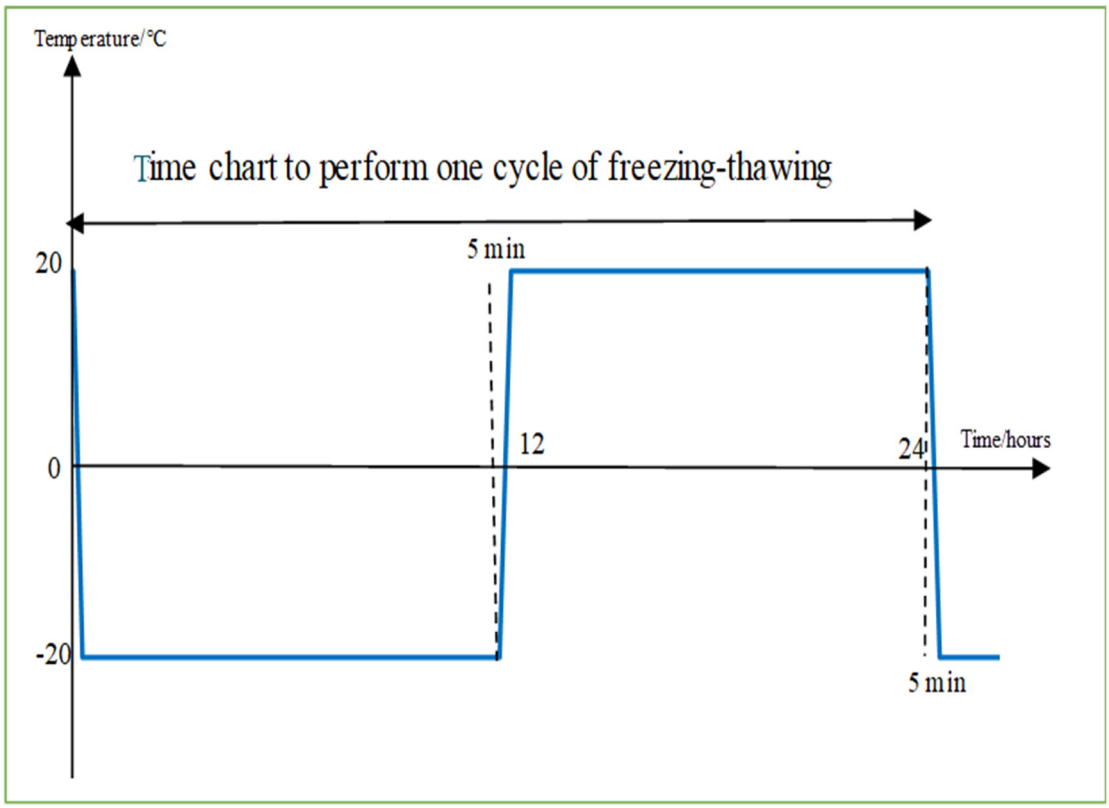

Fig. 8 Schematic diagram of temperature variations in an FT cycle

conducting the defined cycles of F-T. Fig. 6 presents the prepared samples to conduct physical and mechanical tests.

$$I_s = \frac{P}{D_e^2} \quad (5)$$

where P and D_e are the load of failure (KN) and equivalent core diameter.

3.8 F-T process

In this section, an actual environment of mine has been simulated in laboratory condition for conducting the F-T test. Indeed, the case study is covered by snow about 190 days in a year (Fig. 7). Also, air temperature decreases below -20°C in winter. To simulate the real condition of the

area, samples are first submerged in the water for 48 h. Next, they are taken into the freezer at -20°C for 12 h. Finally, specimens were placed in the water bath with a +20°C temperature for 12 h. Accordingly, every cycle of the F-T process takes about 24 h (Fig. 8). The mentioned 5 min in Fig. 8 is the required time to transfer the samples from the freezer to the water bath.

3.9 Decay function model

The impact of N on the deprecation of integrity and durability of rock can be examined using the decay function. This function was first suggested by Mutlutürk *et al.* (2004). The decay function is comprised of half-life ($N_{1/2}$) and decay constant (λ) variables to show the integrity reduction rate of rocks. In the F-T process, the integrity loss rate represents linear direct relation with rock mass integrity in each cycle initiating. Mathematically form of the above relation is prepared as follows

$$-(dI/dN) = \lambda I \tag{6}$$

where (dI/dN) is the rate of disintegration, λ is the decay coefficient, I is the rock integrity, and N is described before. In Eq. (6), the minus symbol show decreasing in rock integrity.

The logarithmic form of Eq. (6) can be calculated as follows

$$\ln(\frac{I_0}{I_N}) = \lambda N \tag{7}$$

In Eq. (7), I_o is the rock's primary integrity and I_N is the rock integrity after N cycles of F-T. Exponential representation of Eq. (7) is

$$I_N = I_0 e^{-\lambda N} \tag{8}$$

The decay factor ($e^{-\lambda N}$) in Eq. (8), shows the remaining integrity proportion after N repetition of the F-T process, i.e., (I_N/I_0). The decay constant (λ) represents the average loss of integrity of the rock due to applying any single cycle of F-T. Also, the rock half-life ($N_{1/2}$) is the specified cycle's number required for decreasing the integrity to its half value. Actually, this factor has an inverse relation to the decay constant. Finally, by the substitution of I_N by ($I_0/2$) in Eq. (7), it can be calculated as follows

$$N_{1/2} = \ln 2 / \lambda \approx 0.693 / \lambda \tag{9}$$

Using the integrity by measuring of decay factor, decay constant, and half-life in the designing phase of engineering projects can provide practical information on rock behavior under various F-T process cycles and leads to technical and optimal design .So, in this study ($N_{1/2}$), λ, and ($e^{-\lambda N}$) were measured for mechanical properties such as point load strength ($I_{S(50)}$), second durability index (Id_2), Brazilian tensile strength (BTS), and compressive (V_P) and shear (V_S) wave velocities, to determining the integrity loss rate for various rock types.

Table 2 Percentages of main rock minerals of the studied samples

Sample No.	Chlorite (%)	Quartz (%)	Calcite (%)	Biotite (%)	Etc (%)
1	15	25	40	20	-
2	10	20	35	25	10
3	15	20	30	25	10
4	20	20	30	20	10

4. Results and discussion

In this section, the mineralogical compositions and structural properties of four samples are first investigated using X-ray diffraction (XRD) and scanning electron microscopy (SEM) analyses. Then changes in physical parameters of calc-schist rock and mechanical characteristics of calc-schist, amphibolite schist, and limestone samples are examined with increasing of N. Finally, the durability of all above-mentioned three rock types is compared by calculating the integrity loss rate of mechanical properties.

4.1 Petrographic study

Petrographic characteristics provided a good information about the mineralogical composition of rocks. Also, studying the rock petrographic characteristics can be an excellent technique to examine the rock stability against the weathering factors, i.e., the F-T process (Jamshidi *et al.* 2013). In this study, the mineralogical properties and petrographic characteristics of two prepared calc-schist specimens were studied using the XRD method and optical microscopy. The results indicate that the calc-schist samples mainly consist of key minerals including calcite, quartz, chlorite, and biotite (Fig. 9). The XRD analysis confirmed the mineral composition obtained from the mineralogical and petrographic analysis of the thin sections. The percentages of the main rock minerals for 4 different samples were detected and shown in Table 2.

4.2 SEM analysis

In this study, variations of microscopic structures of calc-schist samples after specific F-T cycles were analyzed using the SEM analysis. The obtained results (Fig. 10) highlight the difference between the microstructure surface of intact rock and highly weathered rock (after applying 75 F-T cycles). According to these images, microstructures of the rock context after weathering represent some basic variations. For example, the density of the pores is increased, existing discontinuities are expanded, and cohesion between minerals is decreased. Indeed, the high expandability of calcite in the body of the sample causes the initiation of new voids and discontinuity, and expands the available discontinuities. Also, the calc-schist matrix contains about 22.5% biotite as a low-resistance mineral against the weathering. Also, water expansion occurs in the joints and bedding interfaces due to the freezing process

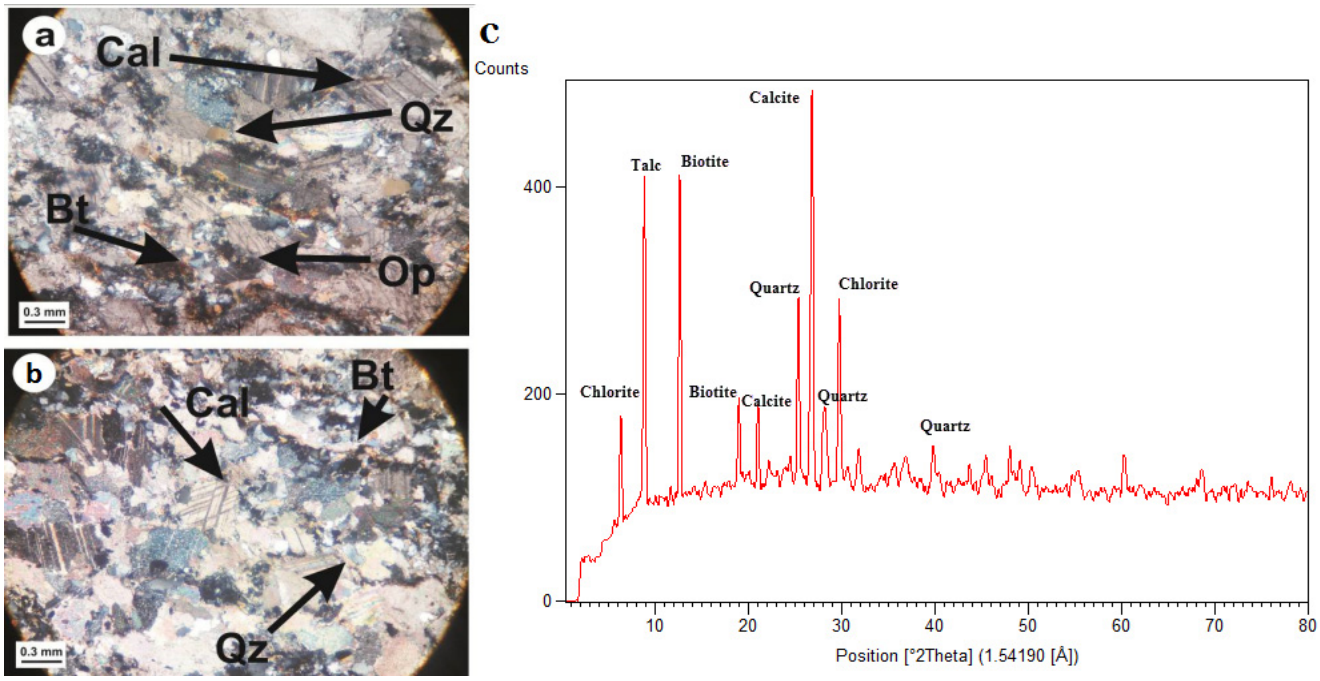

Fig. 9 Results of the petrographic study for two studied samples: (a) & (b) Thin section images and (c) XRD analyses

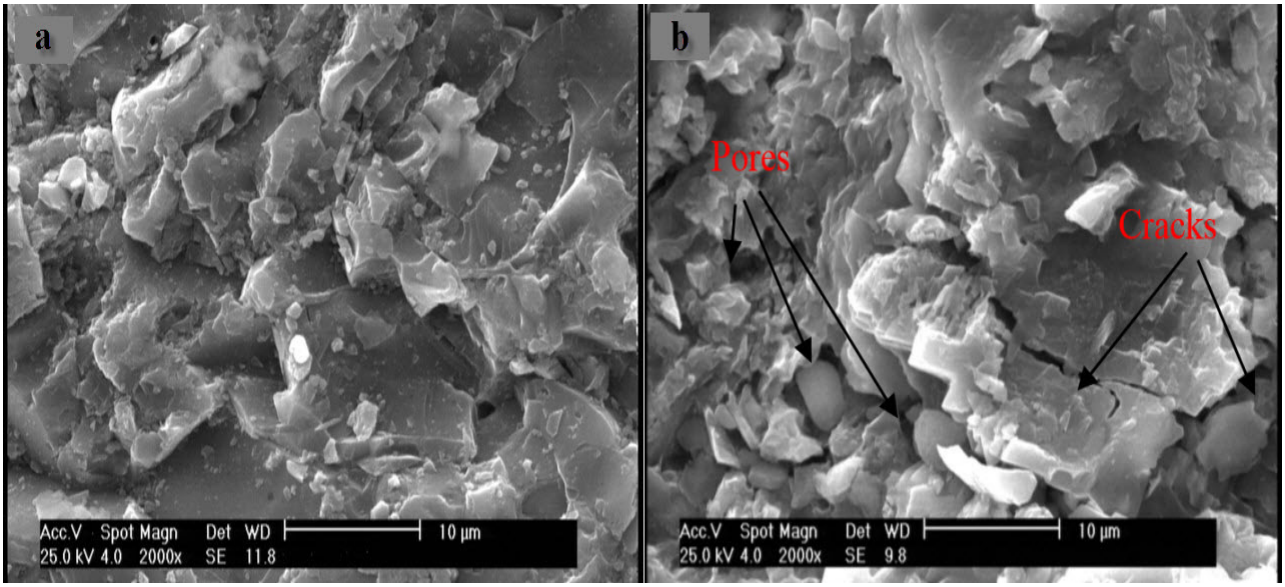

Fig. 10 SEM image of the sample: (a) Intact and (b) After applying 75 cycles of F-T

during the repetition of N. This process causes the creation of new micro-fissures along with the expansion of available cracks. Also, granular minerals can be separated from each other due to this process.

4.3 Physical characteristics

Key physical characteristics of calc-schist rock samples, including porosity (ϕ), dry density (γ_d), and water absorption (W), were determined according to the ISRM (1981), ASTM (2001), and ISRM (2007). Next, the 75 N was applied to the samples, and their γ_d, ϕ, and W were characterized. Indeed, samples characteristics i.e., γ_d, ϕ, and W were measured after 0, 7, 15, 40, and 75 N. The results of conducted tests on dry density, porosity, and water absorption of the specimens are given in Table 3. As it is observed, dry density values are reduced with increasing the N, while water absorption and porosity are increased. Indeed, the density of discontinuity and pores increases when the weathering grade rises. This leads to the loss of density and increases the rock porosity. Besides, the contact area between the rock and water is increased with increasing the number of discontinuity and rock degradation and calcite minerals are further influenced with the increasing of N.

Table 3 The variations in dry density, porosity, and water absorption due to F-T cycles

N	γ_d (gr/cm3)			ϕ (%)			W (%)		
	Max	Min	Mean	Max	Min	Mean	Max	Min	Mean
0	2.69	2.34	2.55	2.74	2.35	2.51	2.36	1.88	2.12
7	2.68	2.35	2.54	2.79	2.49	2.52	2.35	1.85	2.12
15	2.69	2.31	2.54	2.85	2.32	2.54	2.51	2.06	2.16
40	2.65	2.28	2.47	3.34	2.47	2.79	2.76	2.03	2.32
75	2.56	2.21	2.31	4.52	3.21	3.71	4.07	2.45	3.26

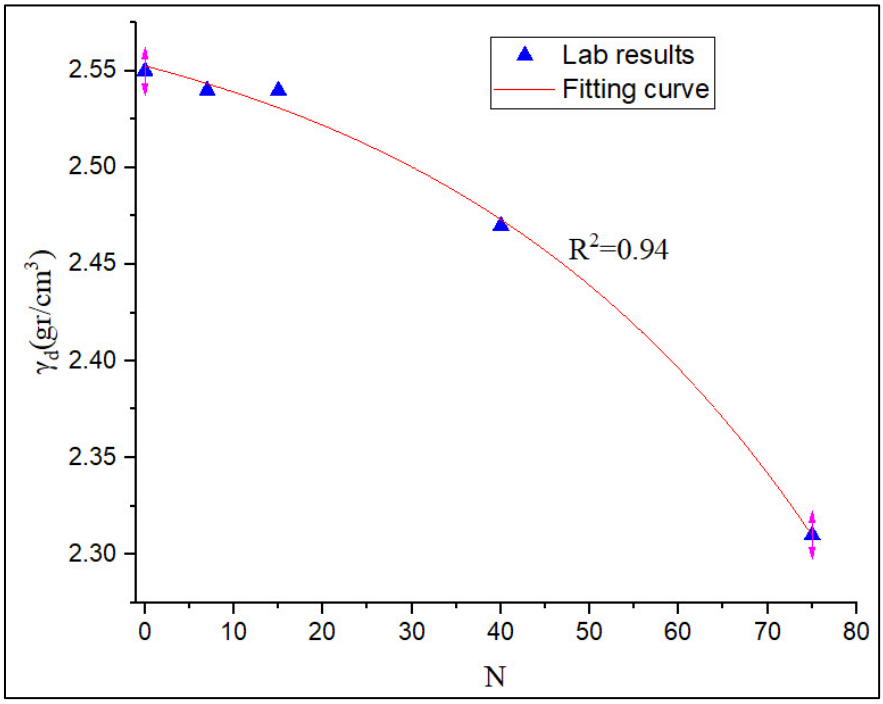

Fig. 11 Changes in dry density with N increasing

Variations of dry density versus N are represented in Fig. 11. As it is observed, the dry density of calc-schist samples is reduced exponentially with increasing the weathering grade. In Figs. 12 and 13, changes in porosity and water absorption are shown against the increasing of weathering grade (increasing the N). These figures showed that N increasing can also cause an exponential increase in porosity and water absorption. Porosity was increased due to the creation of new micro-cracks and expanding the existing cracks. In addition, the water absorption is increased due to the increase in the contact surface of the water and the discontinuity walls because of the further crushing after increasing the weathering grade. Indeed, changes in rock properties occur both linearly and exponentially. This is due to the difference in weathering intensity in the primary and last cycles of F-T. In fact, the strength properties of the sample are degraded slowly (linearly) in the primary cycles of the weathering process. With increasing the weathering cycles, the number of discontinuities is increased and weak minerals are more influenced by the absorbed water and other weathering agents. Hence, the degradation of rock mass properties occurs sharply (exponentially).

4.4 Mechanical characteristics

The relation of N with rock mechanical characteristics including point load strength ($I_{S(50)}$), second durability index (Id_2), Brazilian tensile strength (BTS), and compressive (V_P) and shear (V_S) wave velocities of calc-schist samples are examined here. Then, degradation rate of these parameters was determined due to the F-T process. In addition, these mechanical properties were measured also for amphibolite schist and limestone specimens. The main issue is eventually the comparison of the durability of these rocks that make up the final pit wall of the Angouran mine, under different Ns.

In Table 4, the maximum, minimum, and mean values of the mechanical parameters of calc-schist samples are presented for different F-T cycle numbers. After 75 N, the BTS, I_s, I_{d2}, V_p and V_s are decreased about 42%, 30%, 17%, 22%, and 27%, respectively. As can be seen, the highest reduction is related to the tensile strength parameter. Also, the mechanical characteristics of limestone samples for specific N values were measured and presented in Table 5. As it is obvious, BTS, I_s, I_{d2}, V_p, and V_s are decreased about 23%, 19%, 14%, 18%, and 26%, respectively. According to

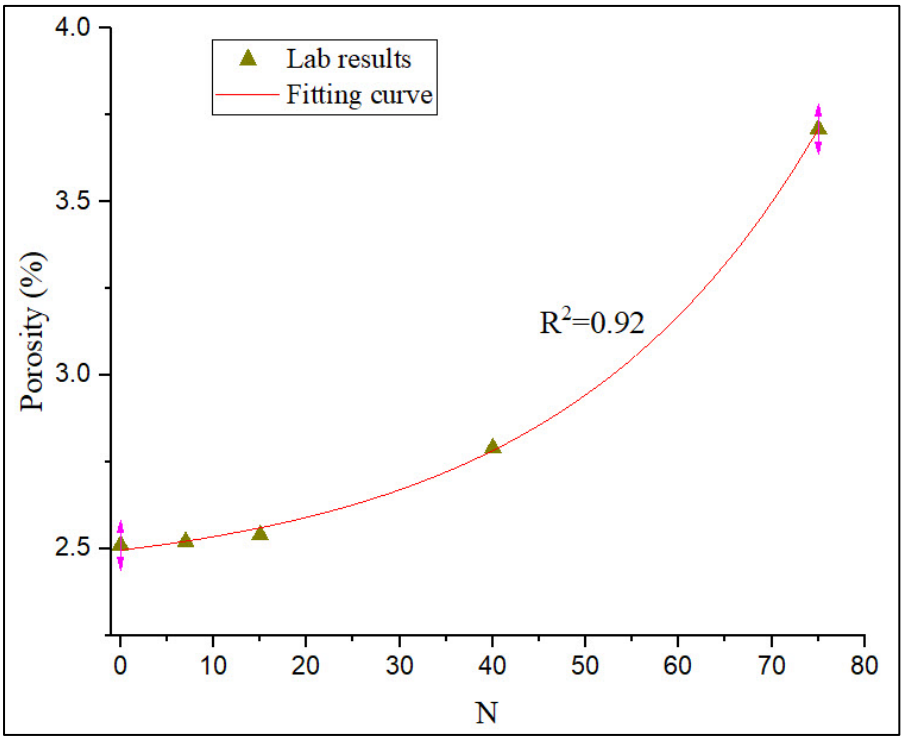

Fig. 12 Changes in porosity with N increasing

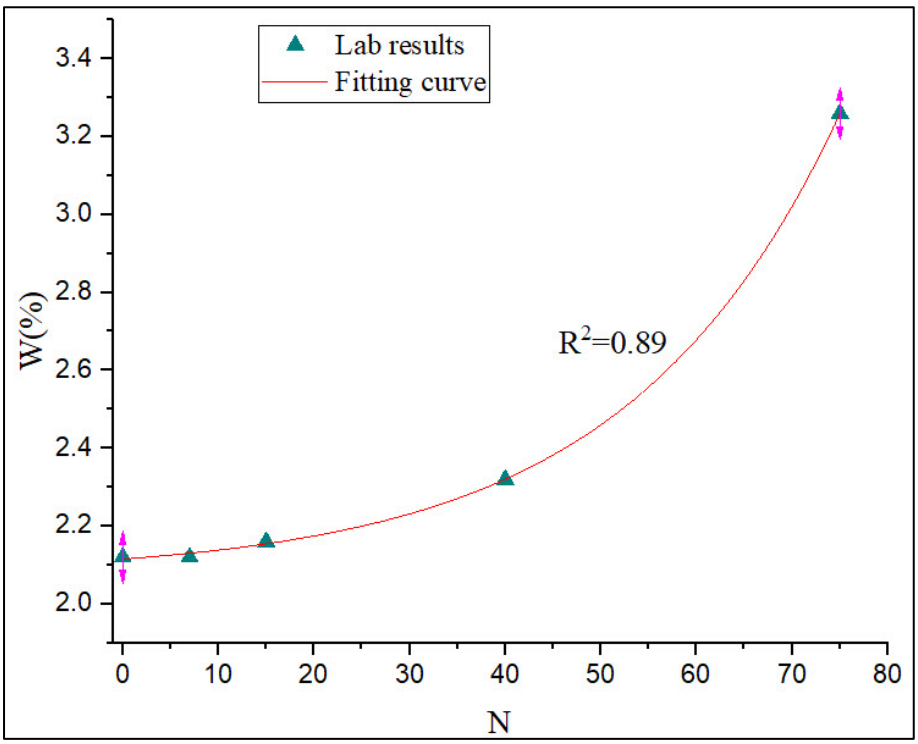

Fig. 13 Changes in water absorption with N increasing

the obtained results, V_s indicates the highest reduction. Finally, the mechanical characteristics of amphibolite rock specimens in different Ns have been determined and given in Table 6. For amphibolite samples, BTS, I_s, I_{d2}, V_p, and V_s are decreased about 12%, 16%, 5%, 12%, and 13%, respectively.

Results indicated that calc-schist specimens involved most degradation rate. The main factor of this degradation is related to existing the loose structures (schistosity and foliation) and weak minerals such as calcite, biotite, and chlorite in their matrix. In addition, the mechanical properties of Amphibolite schist samples are less affected

Table 4 Variations of mechanical properties of calc-schist samples in different F-T cycles

N	$I_{s(50)}$ (MPa)			BTS (MPa)			I_{d2} (%)			V_p (m/s)			V_s (m/s)		
	Max	Min	Mean	Max	Min	Mean	Max	Min	Mean	Max	Min	Mean	Max	Min	Mean
0	2.34	1.45	1.78	4.43	3.25	3.67	99.35	98.02	98.52	4214	3954	4043	2953	2817	2875
7	2.31	1.52	1.80	4.38	3.17	3.74	99.45	98.05	98.15	4147	3967	4035	3018	2825	2890
15	2.23	1.24	1.63	4.18	3.03	3.62	98.83	96.32	97.11	4015	3748	3897	2897	2804	2842
40	1.95	1.05	1.45	3.45	1.97	2.54	98.86	95.17	96.45	3854	3711	3803	2788	2514	2653
75	1.72	0.88	1.24	2.84	1.65	2.11	89.14	75.72	82.12	3257	2984	3154	2247	1913	2087

Table 5 Variations of mechanical properties of limestone samples in different F-T cycles

N	$I_{s(50)}$ (MPa)			BTS (MPa)			I_{d2} (%)			V_p (m/s)			V_s (m/s)		
	Max	Min	Mean	Max	Min	Mean	Max	Min	Mean	Max	Min	Mean	Max	Min	Mean
0	3.54	3.04	3.21	5.53	4.16	4.85	99.87	98.45	98.85	4041	3789	3878	2794	2681	2741
7	3.31	2.89	3.15	5.61	4.22	4.77	99.72	98.34	98.14	3865	3641	3714	2813	2692	2716
15	3.38	2.77	3.08	4.97	3.89	4.54	97.34	94.21	95.14	3798	3662	3721	2751	2576	2667
40	3.14	2.51	2.85	4.81	3.82	4.32	93.54	88.43	90.24	3629	3507	3568	2567	2341	2415
75	2.76	2.13	2.46	4.57	3.36	3.94	90.12	81.27	84.65	3314	3023	3184	2234	1918	2017

Table 6 Variations of mechanical properties of amphibolites samples in different F-T cycles

c	$I_{s(50)}$ (MPa)			BTS (MPa)			I_{d2} (%)			V_p (m/s)			V_s (m/s)		
	Max	Min	Mean	Max	Min	Mean	Max	Min	Mean	Max	Min	Mean	Max	Min	Mean
0	4.95	4.24	4.45	7.66	6.05	6.44	99.93	99.14	99.45	4871	4616	4745	3521	3341	3415
7	4.88	4.06	4.36	7.12	5.83	6.25	99.86	99.17	99.42	4861	4715	4801	3412	3264	3358
15	4.61	4.13	4.25	7.15	5.61	6.18	99.52	98.67	99.13	4736	4552	4654	3451	3227	3334
40	4.45	3.86	4.11	6.62	5.29	6.03	98.69	97.45	98.12	4594	4461	4512	3329	3174	3245
75	4.21	3.25	3.74	6.11	4.94	5.65	96.23	93.79	94.45	4319	4028	4154	3088	2874	2957

by the F-T process compared to the calc-schist and limestone rock specimens. This rock type is a dark-colored rock with hornblende as its major mineral that formed under moderate to high temperature (over 500°C) and pressure. Therefore, amphibolite is poorly foliated and less affected by the schistosity plane (than schist rocks). So, Amphibolite facies condition increases the durability of this rock against F-T process agents. The presence of high calcite amount in the mineralogical composition and high discontinuity planes (schistosity, foliation, and pores) have the most impact on the degradation rate.

Variations of mechanical characteristics as the function of N for all three studied rock types are shown in Figs. 14-18. According to the exponential fitting curve, the decay constant and fit degree of the studied mechanical parameters (BTS, I_s, I_{d2}, V_p, and V_s) for each type of studied rocks are determined and presented in Table 7.

The results showed that rock type has an important impact on the integrity rate of mechanical parameters. According to the calculated correlation coefficient (R), prediction of BTS and I_s was possible with high capability after specific F-T cycles. Also, calc-schist has lower resistance against the F-T cycles compared to the limestone and amphibolite schist samples. For example, $I_{S(50)}$ losses about 30.3%, 23.40%, and 15.95% after 75 cycles of F-T for schist, limestone, and amphibolite schist specimens, respectively. Also, V_s decreased by about 13.4%, 26.4%, and 27.4% for schist, limestone, and amphibolite schist samples, correspondingly. As previously mentioned, this difference is due to the existence of main rock minerals and structures in the rock body. When the main minerals of rock (i.e., calcite, biotite, and clay) have low resistance against the weathering factors, variations slope of the mechanical change curves would be more. Also, the existence of weak structures such as schistosity, foliation, and layering, accelerates the rock degradation amount in the period of the F-T process. Besides, calc-schist is more influenced by F-T cycles than limestone and amphibolite. Since calcite is one of the main minerals of calc-schist, it is easily dissolved in water. Furthermore, other minerals of calc-schist such as biotite and chlorite are more oxidized due to weathering agents over the time.

In the early cycles of F-T, freezing the existing water inside the sample body and its discontinuities, helps the increasing of cracks and pores. As a result, with increasing the temperature and starting the melting process, water flow inside the rock increases which accelerates the degradation loss rate. Also, the lowest degree of integrity loss belongs to the amphibolite schist samples. As it is obvious, the metamorphic faces of amphibolite schist are mainly green schist type. Indeed, amphibolite faces have experienced temperatures of over 500°C and pressures less than 1.2 GPa. So, the density of the schistosity and foliation is reduced. Also, the shear strength of these planes is more than other

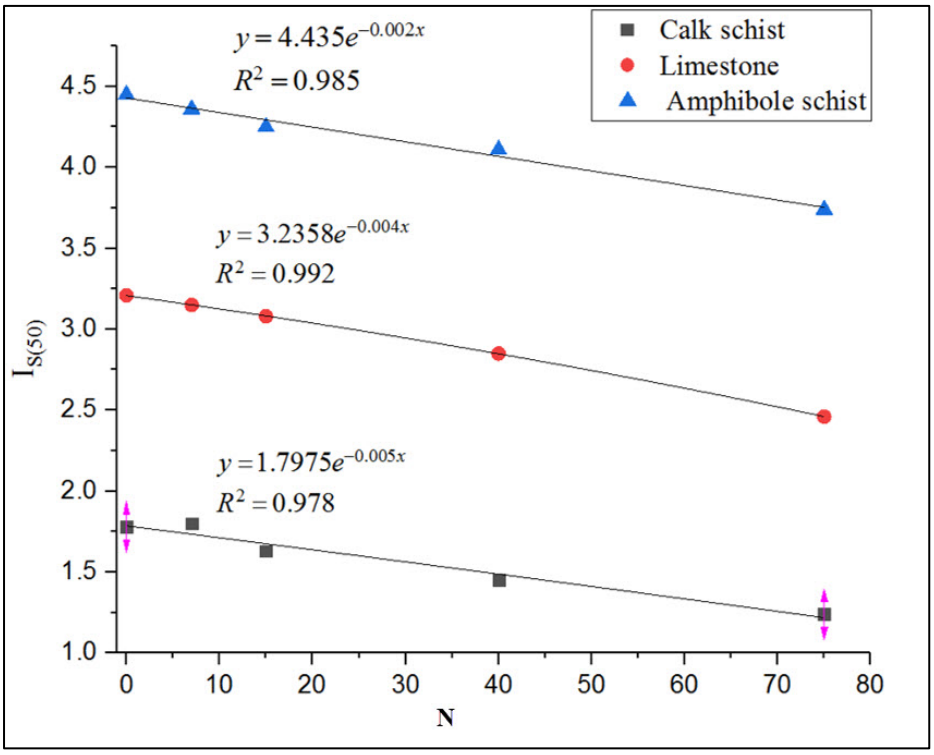

Fig. 14 Variations of point load index ($I_{s(50)}$) vs. N for different rocks

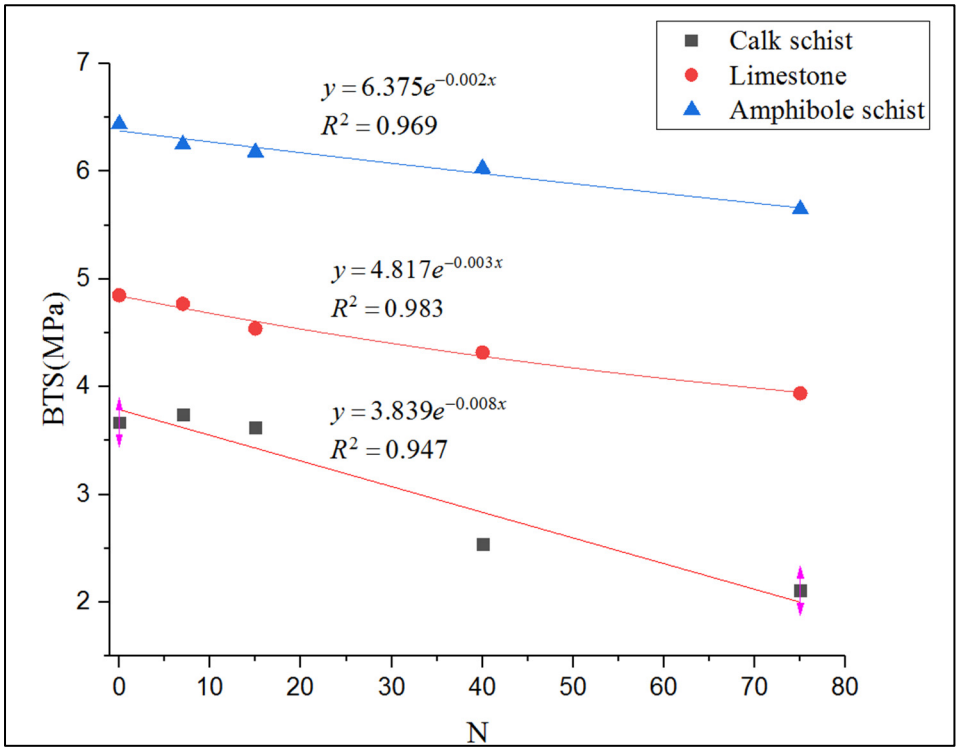

Fig. 15 Variations of Brazilian tensile test (BTS) vs. N for different rocks

schist rocks. As a result, amphibolite schist shows more resistance against weathering factors than the calc-schist. On the other hand, limestone is a mediocre rock and has a dense texture without discontinuities planes but calcite exists in its mineralogical composition.

As previously mentioned, the half-life factor is the main tool to evaluate the rock durability. This parameter is inversely correlated to the decay coefficient. Also, it provides a simple way to estimate the required numbers of F-T cycles to decrease a specified mechanical characteristic

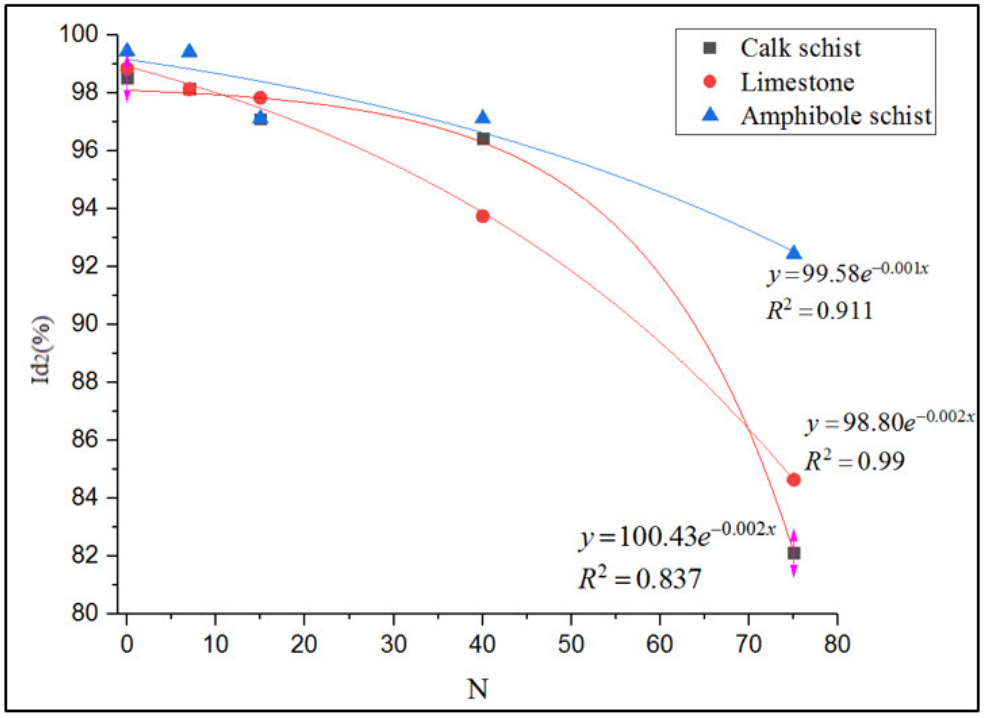

Fig. 16 Variations of second durability index (I_{d2}) vs. N for different rocks

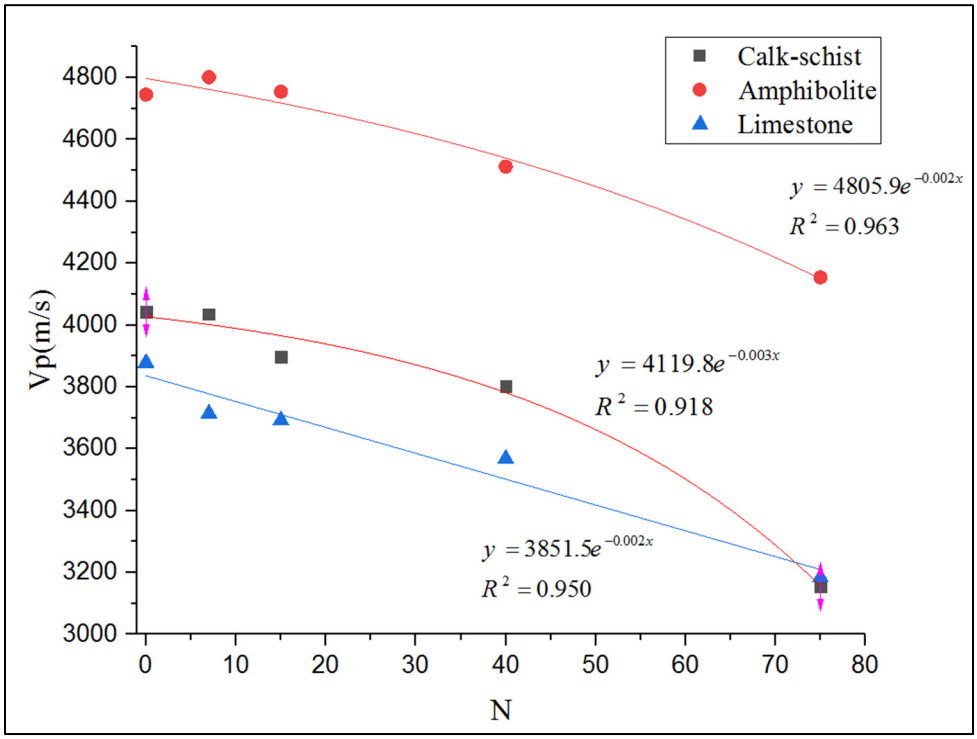

Fig. 17 Variations of compressive wave velocity (Vp) vs. N for different rocks

of rock toward its half value. According to this significance, rocks with more half-life amounts indicated the further resistance against the N and its related instability. The half-life values for each of the studied mechanical characteristics and different rock types were estimated using the decay function (Eq. (9)) and the obtained results are illustrated in Fig. 19. Based on the results of the second durability index, amphibolite schist has the longest half-life (i.e., 693 cycles). Also, the results of point load strength showed that calc-schist has the shortest half-life (i.e., 138.6). In addition, the half-lives vary from 346.5 to 693, 86.625 to 346.5, and 173.25 to 346.5 cycles for amphibolite schist, calc-schist,

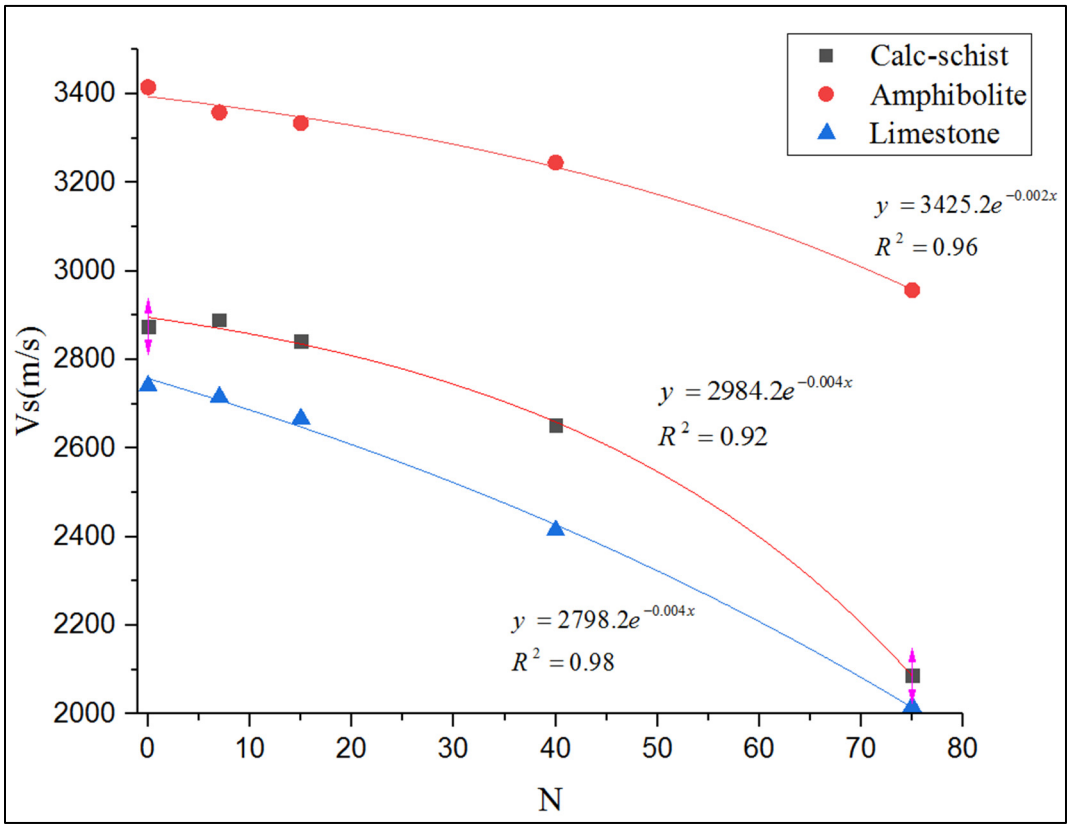

Fig. 18 Variations of shear wave velocity (V_s) vs. N for different rocks

Table 7 Calculating the decay coefficient (λ) and correlation coefficient (R) of mechanical characteristics considering the F-T processes for different rocks

Characteristics	Rock type	R^2	λ
BTS	Calc-schist	0.969	-0.008
	Amphibole schist	0.983	-0.002
	Limestone	0.947	-0.003
Is	Calc-schist	0.963	-0.005
	Amphibole schist	0.992	-0.002
	Limestone	0.978	-0.004
I_{d2}	Calc-schist	0.837	-0.002
	Amphibolite schist	0.911	-0.001
	Limestone	0.99	-0.002
Vp	Calc-schist	0.918	-0.003
	Amphibole schist	0.963	-0.002
	Limestone	0.95	-0.002
Vs	Calc-schist	0.92	-0.004
	Amphibole schist	0.96	-0.002
	Limestone	0.98	-0.004

and limestone, respectively. Finally, based on the achieved outputs, it can be concluded that amphibolite rock is more durable against the weathering process compared to calc-schist and limestone. So these results can help the designing of overall slope angle of final pit walls in considered rocks.

5. Conclusions

In this study, variations of the physical and mechanical characteristics of calc-schist rock were evaluated against the F-T cycles. XRD and SEM analyses were performed for evaluating the strength of rock specimens against the F-T processes. Finally, the long-term durability of calc-schist, limestone, and amphibolite schist against the number of F-T cycles was studied using the decay function and half-time technique. These techniques are key tools to estimate the durability of rock under weathering agents. So, the decay coefficient/constant and half-life elements were determined based on the changes of I_s, BTS, I_{d2}, V_p, and V_s parameters for calc-schist, limestone, and amphibolite schist specimens. The results of the decay function and half-time techniques exposed the sensitivity of these parameters and rock kinds to the F-T process. Overally, the major conclusions of the current research are outlined as the following arrangements:

- The high content of calcite and more schistosity density lead to less durability of calc-schist compared to the amphibolite schist, under weathering agents.
- With N increasing, dry density was decreased, whereas, the porosity and water absorption were increased.
- SEM analyses confirmed that the pressure of freezing in discontinuities wall leads to the creation of new micro-cracks or pores and expands the available discontinuities. Also increasing the temperature and melting the available ice in the rock body causes

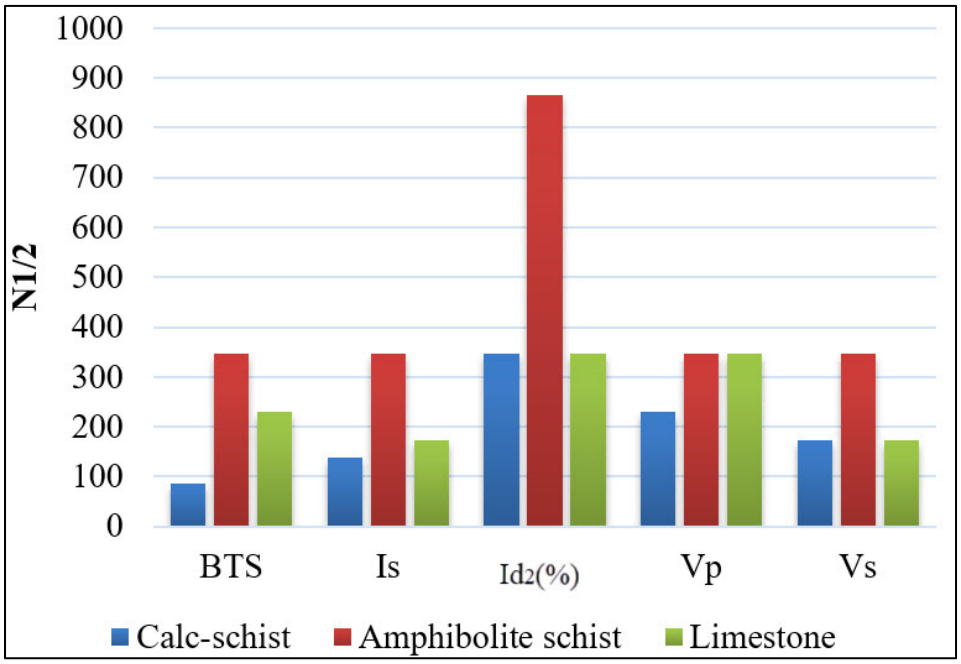

Fig. 19 Amounts of mechanical characteristics half-life of calc-schist, limestone, and amphibolite schist

increasing the water flow into the rock body. So, samples deteriorated during the F-T process cycles.

- Calc-schist specimens were more affected by F-T cycles than limestone and amphibolite schist samples. This is related to calcite content in the mineralogical composition of the calc-schist. Calcite has higher expansion coefficients and it is less resistant to temperature changes than other minerals. Also, the high percentage discontinuities including foliation and schistosity in the rock structure help to more degradation of this rock against weathering factors.
- The results showed an excellent correlation among the elements of the decay function technique and proved that mechanical characteristics of rocks are decreased when they subjected to the F-T cycles.
- The highest and lowest half-lives were calculated for amphibolite schist and calc-schist specimens, respectively.
- As a general result, it is concluded that the long-term permanence prediction of three various rocks in this paper can help a good-decision making in the selection of the overall slope angle of walls and bench face angle in each of the above-unreconstructed rock types.

Acknowledgments

The authors would like to express their thanks to the Angouran mine staff and the rock mechanics laboratory managers of the Shahid Bahonar University of Kerman, the University of Kurdistan, and Amirkabir University of Technology for their supports during the sample preparation and testing.

References

Altindag, R., Alyildiz, I.S. and Onargan, T. (2004), "Mechanical property degradation of ignimbrite subjected to recurrent freeze-thaw cycles", *Int. J. Rock Mech. Min.*, **41**(6), 1023-1028. https://doi.org/10.1016/j.ijrmms.2004.03.005.

Asadizadeh, M. and Rezaei, M. (2021) "Surveying the mechanical response of non-persistent jointed slabs subjected to compressive axial loading utilising GEP approach", *Int. J. Geotech. Eng.*, **15**(10), 1312-1324. https://doi.org/10.1080/19386362.2019.1596610.

ASTM (2001), "*Standard test method for density, relative density (specific gravity), and absorption of coarse aggregate*", ASTM International, Annual Book, USA.

Binal, A., Kasapoglu, K.E. and Gokceoglu, C. (1984), "Variation of some physical and mechanical properties of the volcano-sedimentary rocks around Eskisehir–Yazilikaya under freezing–thawing effect", *Earth Sci. J.*, **20**, 41-54.

Cheng, S., Wang, Q., Fu, H., Wang, J., Han, Y., Shen, J. and Lin, S. (2021), "Effect of freeze-thaw cycles on the mechanical properties and constitutive model of saline soil", *Geomech. Eng.*, **27**(4), 309-322. https://doi.org/10.12989/gae.2021.27.4.309.

Franklin, J.A. and Chandra R. (1972), "The slake durability test". *Int. J. Rock Mech. Min. Sci.*, **9**(3), 325-328. https://doi.org/10.1016/0148-9062(72)90001-0.

Gamble, J.C. (1971), "*Durability-plasticity classification of shales and other argillaceous rocks*". PhD Thesis, University of Illinois Urbana-Champaign, Champaign, IL, United States.

Han, T., Shi, J. and Cao, X. (2016), "Fracturing and damage to sandstone under coupling effects of chemical corrosion and freeze–thaw cycles", *Rock Mech. Rock Eng.*, **49**(11), 4245-4255. https://doi.org/10.1007/s00603-016-1028-7.

Huang, S., Liu, Q., Cheng, A. and Liu, Y. (2018), "A statistical damage constitutive model under freeze-thaw and loading for rock and its engineering application", *Cold Reg. Sci. Technol.*, **145**, 142-150. https://doi.org/10.1016/j.coldregions.2017.10.015.

ISRM (1981), "*Rock Characterization, Testing and Monitoring: ISRM Suggested Methods*", Pergamon Press, Oxford, USA.

ISRM (2007) "*The Complete ISRM Suggested Methods for Rock*

Characterization, Testing and Monitoring: 1974-2006", Suggested Methods Prepared by the Commission on Testing Methods, International Society for Rock Mechanics, Compilation Arranged by the ISRM Turkish National Group Ankara, Turkey, 628 p.

Jamshidi, A., Nikudel, M.R. and Khamehchiyan, M. (2013), "Predicting the long-term durability of building stones against freeze – thaw using a decay function model", *Cold Reg. Sci. Technol*., **92**, 29-36. https://doi.org/10.1016/j.coldregions.2013.03.007.

Jamshidi, A., Reza, M. and Khamehchiyan, M. (2016), "Evaluation of the durability of Gerdoee travertine after freeze–thaw cycles in fresh water and sodium sulfate solution by decay function models". *Eng. Geol*., **202**, 36-43. https://doi.org/10.1016/j.enggeo.2016.01.004.

Karaca, Z., Hamdi, A., Elci, H. and Pamukcu, C. (2010), "Effect of freeze–thaw process on the abrasion loss value of stones". *Int. J. Rock Mech. Min. Sci*., **47**(7), 1207-1211. https://doi.org/10.1016/j.ijrmms.2010.07.003.

Ke, B., Zhou, K., Xu, C., Deng, H., Li, J. and Bin, F. (2018), "Dynamic mechanical property deterioration model of sandstone caused by freeze–thaw weathering", *Rock Mech. Rock Eng*., **51**(9), 2791-2804. https://doi.org/10.1007/s00603-018-1495-0.

Khanlari, G. and Abdilor Y. (2015), "Influence of wet–dry, freeze–thaw, and heat–cool cycles on the physical and mechanical properties of Upper Red sandstones in central Iran", *Bull. Eng. Geol. Environ*., **74**(4), 1287-300. https://doi.org/10.1007/s10064-014-0691-8.

Liu, C., Deng, H., Chen, X., Xiao, D. and Li, B. (2020), "Impact of Rock Samples Size on the Microstructural Changes Induced by Freeze–Thaw Cycles". *Rock Mech. Rock Eng*., **53**, 5293-5300. https://doi.org/10.1007/s00603-020-02201-4.

Moon, J.S., An, J.W., Kim, H.K., Lee, J.G. and Lattner, T. (2022), "Evaluation criteria for freezing and thawing of tunnel concrete lining according to theoretical and experimental analysis", *Geomech. Eng*., **29**(3), 349-357. https://doi.org/10.12989/gae.2022.29.3.349.

Mutlutürk, M., Altindag, R. and Türk, G. (2004), "A decay function model for the integrity loss of rock when subjected to recurrent cycles of freezing-thawing and heating-cooling". *Int. J. Rock Mech. Min. Sci*., **41**(2), 237-244. https://doi.org/10.1016/S1365-1609(03)00095-9.

Rezaei, M. (2018) "Indirect measurement of the elastic modulus of intact rocks using the Mamdani fuzzy inference system", *Measurement*, **129**, 319-331. https://doi.org/10.1016/j.measurement.2018.07.047.

Rezaei, M. (2020) "Feasibility of novel techniques to predict the elastic modulus of rocks based on the laboratory data", *Int. J. Geotech. Eng*., **14**, 25-34. https://doi.org/10.1080/19386362.2017.1397873.

Rezaei, M. and Asadizadeh, M. (2020) "Predicting unconfined compressive strength of intact rock using new hybrid intelligent models", *J. Min. Environ.*, **11**(1), 231-246. https://doi.org/10.22044/JME.2019.8839.1774.

Rezaei, M. and Ghasemi, M. (2023) "An integrated geo-statistical methodology for an optimum resource estimation of angouran underground mine", *J. Min Environ.*, **14**(2), https://doi.org/10.22044/jme.2023.12710.2308.

Rezaei, M. and Nyazyan, N. (2023), "Assessment of effect of rock properties on horizontal drilling rate in marble quarry mining: field and experimental studies", *J. Min. Environ.*, **14**(1), 321-339. https://doi.org/10.22044/jme.2023.12595.2287.

Rezaei, M., Koureh Davoodi, P. and Najmoddini, I. (2019), "Studying the correlation of rock properties with P-wave velocity index in dry and saturated conditions", *J. Appl. Geophy*., **169**, 49-57. https://doi.org/10.1016/j.jappgeo.2019.04.017.

Ruedrich, J., Kirchner, D. and Siegesmund, S. (2011), "Physical weathering of building stones induced by freeze-thaw action: A laboratory long-term study". *Environ. Earth Sci*., **63**(7), 1573-1586. https://doi.org/10.1007/s12665-010-0826-6.

Sardana, S., Sinha, R.K., Verma, A.K. and Singh, T.N. (2022), "Investigations into the freeze–thaw-induced alteration in microstructure and deteriorative responses of physico-mechanical properties of Himalayan rock", *Bull. Eng. Geol. Environ.*, **81**(7), 269. https://doi.org/10.1007/s10064-022-02762-4.

Seyed Mousavi, S.Z. and Rezaei, M. (2022), "Correlation assessment between degradation ratios of UCS and non-destructive properties of rock under freezing-thawing cycles", *Geoderma*, **428**, 116209. https://doi.org/10.1016/j.geoderma.2022.116209.

Seyed Mousavi, S.Z., Tavakoli, H., Moarefvand, P. and Rezaei, M. (2019), "Assessing the effect of freezing-thawing cycles on the results of the triaxial compressive strength test for calc-schist rock". *Int. J. Rock Mech. Min. Sci*., **123**, 104090. https://doi.org/10.1016/j.ijrmms.2019.104090.

Seyed Mousavi, S.Z., Tavakoli, H., Moarefvand, P. and Rezaei, M. (2020), "Micro-structural, petro-graphical and mechanical studies of schist rocks under the freezing-thawing cycles". *Cold Reg. Sci. Technol*., **174**, 103039. https://doi.org/10.1016/j.coldregions.2020.103039.

Takarli, M., Prince, W. and Siddique, R. (2008), "Damage in granite under heating/cooling cycles and water freeze-thaw condition". *Int. J. Rock Mech. Min. Sci*., **45**(7), 1164-1175. https://doi.org/10.1016/j.ijrmms.2008.01.002.

Tan, X., Chen, W., Yang, J. and Cao, J. (2011), "Laboratory investigations on the mechanical properties degradation of granite under freeze–thaw cycles". *Cold Reg. Sci. Technol*., **68**, 130-138. https://doi.org/10.1016/j.coldregions.2011.05.007.

Tang, Z.C., Li, L., Wang, X.C. and Zou, J.P. (2020), "Influence of cyclic freezing-thawing treatment on shear behaviors of granite fracture under dried and saturated conditions". *Cold Reg. Sci. Technol*., **181**, 103192. https://doi.org/10.1016/j.coldregions.2020.103192.

Uğur, İ. and Toklu, H.Ö. (2020) "Effect of multi-cycle freeze-thaw tests on the physico-mechanical and thermal properties of some highly porous natural stones". *Bull. Eng. Geol. Environ*., **79**(1), 255-267. https://doi.org/10.1007/s10064-019-01540-z.

Wang, P., Xu, J., Liu, S., Wang, H. and Liu, S. (2016), "Static and dynamic mechanical properties of sedimentary rock after freeze-thaw or thermal shock weathering", *Eng. Geol*., **210**(4), 148-157. https://doi.org/10.1016/j.enggeo.2016.06.017.

Wang, W., Yang, X., Huang, S., Yin, D. and Liu, G. (2020), "Experimental study on the shear behavior of the bonding interface between sandstone and cement mortar under freeze–thaw". *Rock Mech. Rock Eng*., **53**(7), 881-907. https://doi.org/10.1007/s00603-019-01951-0.

Yavuz, H., Altindag, R., Sarac, S., Ugur, I. and Sengun, N. (2005), "Estimating the index properties of deteriorated carbonate rocks due to freeze-thaw and thermal shock weathering". *Int. J. Rock Mech. Min. Sci*., **43**(5), 767-275. https://doi.org/10.1016/j.ijrmms.2005.12.004.

Yilmaz, F. and Fidan, D. (2018), "Influence of freeze-thaw on strength of clayey soil stabilized with lime and perlite", *Geomech. Eng*., **14**(3), 301-306. https://doi.org/10.12989/gae.2018.14.3.301.

Zhang, J., Deng, H., Deng, J. and Guo, H. (2020) "Influence of freeze-thaw cycles on the degradation of sandstone after loading and unloading". *Bull. Eng. Geol. Environ*., **79**, 1967-1977. https://doi.org/10.1007/s10064-019-01634-8.

CC